

1 **Wetland eco-engineering: measuring and modeling feedbacks of oxidation**  
2 **processes between plants and clay-rich material**

3 Rémon Saaltink<sup>1</sup>, Stefan C. Dekker<sup>1</sup>, Jasper Griffioen<sup>1,2</sup>, Martin J. Wassen<sup>1</sup>

4

5 <sup>1</sup> Department of Environmental Sciences, Copernicus Institute of Sustainable  
6 Development, Utrecht University, Utrecht 3508 TC, The Netherlands.

7 <sup>2</sup> TNO Geological Survey of the Netherlands, Princetonlaan 6, 3584 CB Utrecht, The  
8 Netherlands

9

10 **Corresponding author**

11 Rémon Saaltink

12 e-mail: [r.m.saaltink@uu.nl](mailto:r.m.saaltink@uu.nl)

13 tel: +31 30 253 2404

14

15

16 **Abstract**

17 Interest is growing in using soft sediment as **a foundation** in eco-engineering  
18 projects. Wetland construction in the Dutch lake Markermeer is an example: here  
19 dredging some of the clay-rich lake-bed sediment and using it to construct wetland  
20 will soon **begin**. Natural processes will be utilized during and after construction to  
21 accelerate ecosystem development. Knowing that plants can eco-engineer their  
22 environment via positive or negative biogeochemical plant–soil feedbacks, we  
23 conducted a six-month greenhouse experiment to identify the key biogeochemical  
24 processes in the mud when *Phragmites australis* is used as an eco-engineering  
25 species. We applied inverse biogeochemical modeling to link observed changes in

26 pore water composition to biogeochemical processes. Two months after  
27 transplantation we observed reduced plant growth and shriveling and yellowing of  
28 foliage. The N:P ratios of plant tissue were low and **these** were affected not by  
29 hampered uptake of N, but by enhanced uptake of P. Subsequent analyses revealed  
30 high Fe concentrations in the leaves and roots. Sulfate concentrations rose  
31 drastically in our experiment due to pyrite oxidation; as reduction of sulfate will  
32 decouple Fe-P in reducing conditions, we argue that plant-induced iron toxicity  
33 hampered plant growth, forming a negative feedback loop, while simultaneously  
34 there was a positive feedback loop, as iron toxicity promotes P mobilization as a  
35 result of reduced conditions through root death, thereby stimulating plant growth and  
36 regeneration. Given these two feedback mechanisms, we propose **the use of Fe-**  
37 **tolerant species rather than species that thrive in N-limited conditions**. The results  
38 presented in this study demonstrate the importance of studying the biogeochemical  
39 properties of the **situated sediment** and the feedback mechanisms between plant  
40 and soil prior to finalizing the design of the eco-engineering project.

41

42 **Keywords:** Drying; Fe-P; Iron toxicity; P mobilization; PHREEQC; Pyrite

43

44

## 45 **1. Introduction**

46

47 Nowadays, natural processes are being used across the world to achieve fast  
48 ecosystem development while at the same time providing opportunities for  
49 developing hydraulic infrastructure, a concept called Building with Nature (BwN)  
50 (Temmerman et al., 2013). Though mostly focused on water safety and coastal

51 protection (e.g. Borsje et al., 2011), BwN can also be applied for the management of  
52 fine sediments. A relevant application could be to use soft sediments as material for  
53 building freshwater wetlands. Here, vegetation can be used as an eco-engineer  
54 (Jones et al., 1994), to modify the environment (Lambers et al., 2009). When fine  
55 sediments are used for the construction of wetlands, however, the use of eco-  
56 engineers is anticipated to pose challenges in relation to crest stability, consolidation  
57 and soil formation.

58 **In the Netherlands, a soft, clay-rich lake-bed sediment is causing serious turbidity**  
59 **problems in the Markermeer (an artificial lake of 691 km<sup>2</sup>):** primary productivity is  
60 impeded and biodiversity in the lake is declining (Vijverberg et al., 2011; Noordhuis  
61 et al., 2014). Because the lake is shallow, wind-induced waves frequently induce  
62 high bed shear stress, which causes sediment to be resuspended (Vijverberg et al.,  
63 2011). To improve the ecological conditions in the lake, **plans are underway** to  
64 dredge some of the soft, clay-rich sediment and use it to construct approximately  
65 10,000 ha of wetland.

66 Plants produce root exudates which influence soil formation by enhancing  
67 microbiological activity (Holtkamp et al., 2011), biological weathering and nutrient  
68 cycling (Taylor et al., 2009; Bradford et al., 2013). An example is the ability of plant  
69 roots to mobilize P by ligand exchange and dissolution of Fe-bound P (Fe-P) by  
70 citrate and oxalate excretion (Gerke et al., 2000). Plant roots may also enhance  
71 consolidation processes in substrate by increasing horizontal and vertical drainage  
72 (O'Kelly, 2006).

73 However, both negative and positive plant–soil feedbacks exist, in which the  
74 physical and chemical properties of the soil affect plant development and vice versa  
75 (Ehrenfeld et al., 2005). Therefore, when looking at soil formation, it is important to

76 study the signs and strengths of these plant–soil feedback mechanisms. For  
77 example, nutrient conditions co-determine the type of plant community that develops  
78 (e.g. Olde Venterink, 2011), which in turn influences the nutrient conditions in the soil  
79 itself (Onipchenko et al., 2001). As feedback mechanisms differ between plant  
80 species (Ehrenfeld et al., 2005), it is essential to determine which eco-engineer is  
81 most appropriate for accelerating ecosystem development in these sediments.

82 De Lucas Pardo (2014) found that the Markermeer mud deposits had a high water  
83 content (20–60% of fresh weight) and were largely anoxic, with oxygen present only  
84 in the top 2 mm. Therefore, when such mud is taken from the lake and spread out in  
85 contact with the air, biogeochemical plant–soil processes related to oxidation and  
86 drying of the top soil are expected to play a significant role. Two types of clay-rich  
87 deposits are the intended sediment for the wetland. Their composition is the product  
88 of a combination of historical and present-day factors. Prior to 1932, the year in  
89 which the dam cutting off the Zuiderzee from the North Sea was completed, this was  
90 a marine environment into which several rivers discharged, including a branch of the  
91 river Rhine (the river IJssel). Hence, a near-shore marine deposit underlies the  
92 present-day soft, clay-rich sediment. This soft, clay-rich layer is produced by  
93 bioturbation and physical weathering and continuously resuspends as a result of  
94 wave action (Van Kessel et al., 2008; De Lucas Pardo et al., 2013). This layer  
95 accumulated after 1976, when northward sediment transport was blocked by a  
96 second dam that separated Markermeer from IJsselmeer, thus allowing suspended  
97 matter to resettle on top of the marine deposit. We can therefore distinguish two  
98 layers: an upper disturbed mud layer prone to bioturbation and erosion, and a  
99 relatively undisturbed layer below.

100 We set up an experiment to monitor the chemical composition of pore water to  
101 identify the biogeochemical plant–soil feedback processes that occur when  
102 oxidation, drying and modification by plants alter the biogeochemical conditions of  
103 these two sediment types, thus in turn affecting vegetation development. Our study  
104 has two subsidiary aims: to ascertain how *Phragmites australis* eco-engineer its  
105 environment by expediting biogeochemical processes in the deposits, and to  
106 simulate the geochemical differences between disturbed mud and undisturbed clay  
107 deposits and relate these to the processes identified from the pore water by using  
108 PHREEQC for inverse modeling. In addition, we altered the grain size of the  
109 disturbed mud deposit by adding inert sand to see how grain size distribution  
110 impacts pore water chemistry.

111 Changes in biogeochemical processes that are related to oxidation are expected  
112 to play a major role as *P. australis* is known for its high radial oxygen loss (Brix et al.,  
113 1996; Dickopp et al., 2011; Smith and Luna, 2013). Oxidation of the sediment will  
114 decrease the concentration of phytotoxins typically found in waterlogged soils, such  
115 as iron, and therefore will have a positive effect on plant development. This will be  
116 more pronounced in undisturbed mud, which is largely anoxic, than in disturbed mud,  
117 of which the top layer is already oxidized and where bioturbation modified the  
118 sediment. The type of biogeochemical processes altered will depend on the intrinsic  
119 properties of the different sediment types, which will be examined in this study.

120

121

## 122 2. Material and Methods

### 123 2.1 Set-up

124 A greenhouse experiment was conducted for six months at the test facility of Utrecht  
125 University. A basin of 4 m<sup>2</sup> (2 x 2 m) was filled with artificial rainwater and was  
126 refreshed every two weeks. At regular intervals, the chemistry of the water was  
127 checked to ensure that the water composition remained stable during the  
128 experiment. The artificial rainwater was made by adding 15 µmol NH<sub>4</sub>(SO<sub>4</sub>), 50 µmol  
129 NaNO<sub>3</sub> and 30 µmol NaCl to osmosis water. These values reflect the average  
130 rainwater composition in the Netherlands for the period 2012–2013 (LMRe, 2014).

131 The sediments used include the soft, clay-rich layer (Mud<sub>soft</sub>) and the underlying,  
132 consolidated, Zuiderzee deposit (Clay). In principle, both sediments have the same  
133 origin and were collected in the same area. We also included a third sediment type  
134 (Mud<sub>sand</sub>), as it is expected that Mud<sub>soft</sub> will be too soft for **constructing wetlands**: a  
135 1:1 mixture was made by mixing mud with Dorsilit<sup>®</sup> crystal silica sand (c. 99% SiO<sub>2</sub>)  
136 which had been autoclaved for one hour at 120 °C prior to mixing. **The sand grains of**  
137 **this material are 0.3-0.8 mm in diameter with D50 being 0.57 mm.** The Mud<sub>soft</sub> and  
138 Clay sediments were collected by mechanically dredging in the southern part of the  
139 lake and were stored in air-tight containers at 4 °C prior to the start of the  
140 experiment.

141 Plastic pots (diameter 10 cm, depth 18 cm) with a perforated base were filled to  
142 within 1 cm **from** the top with one of the three sediment types used (t = 0). In each  
143 pot, two soil moisture samplers (Rhizon Flex-5cm; Rhizosphere, Wageningen, the  
144 Netherlands) were installed horizontally at depths of 1 cm and 11 cm below the  
145 sediment surface (these depths are hereafter referred to as D<sub>1</sub> and D<sub>11</sub>), **its tip**  
146 **reaching 5 cm from the pot wall.** The pots were stood in rows in the basin. The water

147 level was maintained at 9 cm so that the sediment at D<sub>11</sub> remained saturated while  
148 the sediment at D<sub>1</sub> could oxidize and dry. Each sediment type had 13 replicates.

149 Reed seedlings (*Phragmites australis*) had been grown in nutrient-poor peat and  
150 when 35–40 days old (experimental time  $t = 22$  days), a single reed seedling was  
151 planted per pot in eight of the replicates, leaving five replicates unplanted. Any other  
152 seedlings that germinated spontaneously in the pots were removed immediately.

153

## 154 2.2 Chemical analysis

155 Soil moisture at D<sub>1</sub> and D<sub>11</sub> was collected from the moisture samplers on days 0, 3,  
156 10, 22, 36, 64, 92, 134 and 174 from five of the pots per condition. The samples from  
157 the five replicates were pooled and chemically analyzed. Chloride, NH<sub>4</sub>, NO<sub>2</sub>, NO<sub>3</sub>  
158 and SO<sub>4</sub> were determined using ion chromatography (IC); Ca, Fe, K, Mn, Na, P, Si  
159 and Sr were determined with Inductively Coupled Plasma Optical Emission  
160 Spectrometry (ICP-OES), pH by an ion-specific electrode, and alkalinity was  
161 measured by a classic titration method.

162 Sediment samples were collected for each sediment type at  $t = 0$  and were freeze–  
163 dried and stored anoxically prior to geochemical analysis. The major elements were  
164 determined using ICP-OES following an aqua regia destruction. Total S content was  
165 measured on an elemental CS analyzer and the mineralogical composition was  
166 determined with X-ray diffraction (XRD). A sequential extraction method based on  
167 Ruttenberg (1992) was applied to characterize solid P speciation. The method  
168 involves five steps (Table 1), the first four of which were carried out anoxically. Loss  
169 on ignition (LOI) was determined by slowly heating to 1000 °C. LOI was also used as  
170 a proxy for organic matter content and total carbonates by calculating the weight loss  
171 between 105–550 °C for organic matter and the weight loss between 550–1000 °C

172 for total carbonates (Howard, 1965). Cation exchange capacity (CEC) of the  
173 sediments was calculated from the organic matter content and the amounts and  
174 types of clay minerals present (Bauer and Velde, 2014).

175 Fifty seedlings of *P. australis* randomly chosen from the seedlings grown for the  
176 experiment were used to determine the initial tissue contents of Fe, K, P, and N.  
177 Their roots, shoots, and leaves were separated and air dried. The air-dried material  
178 was then ground and analyzed with total reflection X-ray fluorescence (TXRF) to  
179 determine tissue contents of Fe, K, and P. Nitrogen content was determined on an  
180 elemental CN analyzer. At the end of the experiment (t = 174), the plants in the pots  
181 were harvested and subjected to the same procedure, to determine the tissue  
182 contents of Fe, K, P, and N.

183

### 184 *2.3 Modeling of biogeochemical processes*

185 To identify important biogeochemical processes during the incubation experiments,  
186 we modeled with PHREEQC (Parkhurst and Apello, 2013). PHREEQC modeling is  
187 frequently used in geochemical research focusing on issues of water quality:  
188 examples include investigating mineral weathering in a mountain river (Lecomte et  
189 al., 2005), deducing geochemical processes in groundwater (Belkhiri et al., 2010)  
190 and investigating the interaction between two aquifers (Carucci et al., 2012). Here,  
191 we applied it to identify biogeochemical plant-soil processes during the oxidation  
192 and natural drying out of the soil.

193 The model approach is based on mass-balance equations of preselected mineral  
194 phases (reactants). The mineral phases can either precipitate (leave the solution) or  
195 dissolve (enter the solution) and these are expressed in mole transfers. As we only  
196 know the dynamics in concentrations of the pore water, we applied inverse modeling



197 in which all possible combinations of the mass-balance equations are accepted  
198 within a range of measured pore water concentrations  $\pm 4\%$ . We can simulate  
199 infiltration or evaporation rates from the pore water. Since in freshwater mud  
200 deposits, the dissolution or precipitation of salts (e.g. NaCl) is negligible and can be  
201 ignored, the change in pore water Cl concentration was used to calculate the amount  
202 of water evaporated or infiltrated.

203 To enable the model to attribute some of the chemical changes to cation-exchange  
204 processes we included an assemblage of exchangers (X):  $\text{CaX}_2$ ,  $\text{FeX}_2$ ,  $\text{KX}$ ,  $\text{MgX}_2$ ,  
205  $\text{NaX}$  and  $\text{NH}_4\text{X}$ . The sum of this assemblage was defined as CEC calculated from  
206 the sediment composition. CEC is important, since it can buffer some of the  
207 biogeochemical processes in sediments by adsorption or desorption of cations.

208 We identified three time frames in our models: 1) oxidation and natural drying out  
209 of the soil before the seedlings were transplanted into the pots ( $t = 0\text{--}22$  days); 2)  
210 initial stage of plant growth ( $t = 22\text{--}64$  days); and 3) the stage in which roots started  
211 to influence pore water chemistry ( $t = 64\text{--}176$  days). These time frames were  
212 identified by analysing the chemical data that was collected. When concentrations at  
213 D11 in the planted condition started to deviate from the unplanted condition, this was  
214 seen as a sign that plant roots started to influence pore water chemistry.

215 Inverse modeling was applied for all combinations (sediment type, plant/no plant,  
216 and depth) for each time frame. For every combination, several valid simulations  
217 were found, due to small differences in the amount of mole transfers attributed to the  
218 mineral phases. Here we present the plausible simulation with the least amount of  
219 mole transfers for each combination.

220

221 **2.4 Statistical analysis**

222 Statistical analysis was carried out using the programs R and SPSS. Differences in  
223 sediment, pore water and plant tissue concentrations between sediment treatments  
224 were determined using one-way ANOVA with a Tukey's honestly significant  
225 difference (HSD) post hoc test. No statistics could be applied to the mineralogical  
226 sediment composition (XRD analysis) due to absence of replicates.

227

228

### 229 **3. Results and Discussion**

230 First, the three sediment types will be compared in terms of certain geochemical and  
231 mineralogical elements. Next, the composition of the pore water will be introduced  
232 and will be linked to biogeochemical processes by presenting and discussing the  
233 PHREEQC model simulations. Then, the plant response is presented and discussed  
234 in terms of biomass and plant tissue chemistry. Lastly, the implications for eco-  
235 engineering will be discussed.

236

#### 237 *3.1 A brief comparison between sediment types*

238 Table 2 shows the geochemical composition of the disturbed Mud<sub>soft</sub> and Mud<sub>sand</sub>  
239 and undisturbed Clay sediments used in this study. The differences between Mud<sub>soft</sub>  
240 and Mud<sub>sand</sub> are solely attributable to the presence of inert Dorsilit®.

241 The total sediment concentrations of Al, Fe, Mg, Mn, Na, P, and Zn were  
242 significantly higher in Clay than in Mud<sub>soft</sub> ( $p < 0.05$ ). The quartz content was also  
243 higher in Clay, which suggests that there were more reactive minerals in this type of  
244 sediment.

245 Sequential P extraction revealed that the significant difference in total P consists of  
246 a significantly lower content of Fe-P in Mud<sub>soft</sub> than in Clay (279 mg/kg versus 772

247 mg/kg;  $p < 0.01$ ); the other P pools did not differ significantly ( $p > 0.11-0.94$ ). The  
248 presence of Fe-P in the anoxic Clay sediment was unexpected, as in anoxic  
249 conditions Fe prefers to bind with S to form  $\text{FeS}_2$ . However, after exhaustion of S,  
250 precipitation of Fe(II) phosphates may occur (Jilbert and Slomp, 2013). Another  
251 possibility is that the reduction of crystalline Fe(III) is not complete in the anoxic  
252 sediment because kinetic processes are slow (Canavan et al., 2007). This is likely  
253 the case in Markermeer, given our strict anoxic procedures for storage and analysis  
254 of the samples. The exchangeable (or loosely sorbed) P was low in Mud<sub>soft</sub> and Clay,  
255 indicating that only a small part of the total P found in the sediments was readily  
256 available for uptake. The other three P-pools were fairly similar and did not differ  
257 significantly between the two types of sediment ( $p > 0.11-0.94$ ).

258 The mineralogical analysis (XRD) showed not only that the quartz content was  
259 lower in Mud<sub>soft</sub> than in Clay (37% versus 48%) but that the amounts of calcite and  
260 pyrite did not differ between the two types of sediment (9% calcite and 0.6% pyrite).  
261 The amount of phyllosilicates (sum of illite, smectite, kaolinite, and chlorite) was  
262 higher in Mud<sub>soft</sub> than in Clay: 43% versus 30%. This must also have caused the  
263 CEC to be higher in Mud<sub>soft</sub>, as the organic matter content did not differ much  
264 between the two (7.2% in Mud<sub>soft</sub> and 6.8% in Clay).

265

### 266 *3.2 Pore water composition*

267 Figure 1 presents time series for the pore water concentrations of the three  
268 macronutrients N, P, and K. The initial decrease in  $\text{NH}_4$  and increase in  $\text{NO}_x$  at a  
269 depth  $D_1$  for the planted conditions was most likely caused by nitrification as a result  
270 of oxidation (Figure 1a–f). At the end of the experiment, almost all dissolved  
271 inorganic nitrogen had been removed from the pore water in the pots with plants,

272 whereas in the pots without plants, the  $\text{NH}_4$  concentrations remained substantial.  
273 Furthermore, a high peak of  $\text{NO}_x$  was observed in Clay sediments at day 10 of the  
274 experiment. At a depth  $D_{11}$ , no large changes were found in general for  $\text{NH}_4$  and  
275  $\text{NO}_x$ .

276 A sharp decline in soluble P was visible at  $D_1$  for all three sediments, probably  
277 because P precipitated with Fe(III) when oxygen penetrated the top layer (Figure 1g–  
278 i). However, in Clay this decline was preceded by an increase in P. After several  
279 weeks, a thin moss layer started to develop on top of the  $\text{Mud}_{\text{soft}}$  sediment, which  
280 probably prevented oxygen from penetrating and thereby increased the P  
281 concentrations (Figure 1g). Similar developments were observed for  $\text{Mud}_{\text{sand}}$   
282 although here the moss layer developed much later. In Clay, no moss grew  
283 throughout the experiment.

284 Concentrations of K were higher than concentrations of N and P and increased in  
285 the first few weeks (Figure 1j–l). No difference was found between pots at  $D_{11}$  with or  
286 without plants. However, K was significantly higher at  $D_1$  in the planted pots with  
287  $\text{Mud}_{\text{sand}}$  ( $p < 0.05$ ).

288 Although it may be important to study measured concentrations of nutrients in pore  
289 water in order to understand plant functioning, deriving biogeochemical processes  
290 from measured data is problematic changes in pore water can be caused by multiple  
291 processes such as drying, dilution, dissolution, and precipitation. Figure 2 reveals  
292 that the drying of soils at  $D_1$  was probably an important factor, because we observed  
293 an initial increase in Cl that indicated that Cl could not dissolve in the three  
294 sediments used (e.g. halite dissolution). Drying will have influenced other variables  
295 as well, such as sulfate (Figure 2d–f). Comparing the patterns of Cl and  $\text{SO}_4$   
296 suggests that the change in  $\text{SO}_4$  concentrations at  $D_1$  should be partly attributed to

297 drying out of soils and partly either to dissolution (e.g. pyrite oxidation) or to  
298 precipitation (e.g. gypsum formation). This highlights the need to use geochemical  
299 reaction models like PHREEQC to inversely derive biogeochemical processes from  
300 measured data.

301

### 302 3.3 Pore water processes (PHREEQC model simulations)

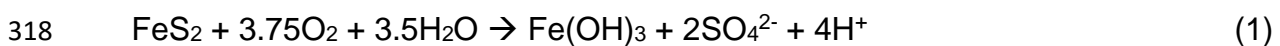
303 The main pore water processes modeled by PHREEQC are presented in Table 3.  
304 For clarity, only major reactants are included in this Table. Supplementary Tables A1  
305 and A2 present mole transfers for all reactants used, as well as the number of valid  
306 simulations per combination found.

307

#### 308 3.3.1 Phase 1: Oxidation and drying (t = 0–22 days)

309 As discussed in section 3.2, initial drying of soils occurred at D<sub>1</sub> immediately after  
310 exposure to air. In the model, this is illustrated by high evaporation rates expressed  
311 as H<sub>2</sub>O loss (2300–3400 mmol l<sup>-1</sup> day<sup>-1</sup>; Table 3). The model accounts for this loss  
312 by adjusting the solution fractions before calculating other mole transfers.

313 Exposure to air also leads to oxidation, more so at D<sub>1</sub> than at D<sub>11</sub> (Table 3). The  
314 increase in measured sulfate is partly explained as pyrite oxidation (109–270 μmol l<sup>-1</sup>  
315 day<sup>-1</sup> for D<sub>1</sub> and 20.1–36.2 μmol l<sup>-1</sup> day<sup>-1</sup> for D<sub>11</sub>, respectively). Oxidation of pyrite  
316 also produces iron oxyhydroxides and protons which in turn promotes dissolution of  
317 calcite. The overall reactions are



319

320 followed by calcite dissolution



322

323 The mole transfers for pyrite and calcite presented in Table 3 indicate that not  
324 enough calcite is dissolved to buffer all H<sup>+</sup> produced by dissolution of pyrite. Indeed,  
325 a drop in pH was observed at the beginning of the experiment (not shown). However,  
326 the mineralogical composition presented in Table 2 shows that the amount of calcite  
327 (9%; 900 mmol) far exceeds that of pyrite (0.6%; 50 mmol). These numbers suggest  
328 that even if all pyrite were to be oxidized, enough calcite is present to buffer all H<sup>+</sup>  
329 produced (200 mmol). Note that for Mud<sub>sand</sub> these values are lower due to mixing  
330 with Dorsilit<sup>®</sup>.

331 Some aeration occurred at D<sub>11</sub>. The O<sub>2</sub> fluxes ranged between 61 and 119 μmol l<sup>-1</sup>  
332 day<sup>-1</sup>, which resulted in small amounts of pyrite being oxidized (20–36 μmol l<sup>-1</sup> day<sup>-1</sup>).  
333 However, sulfate concentrations did not rise, as a result of subsequent precipitation  
334 with Ca to form gypsum (53–73 μmol l<sup>-1</sup> day<sup>-1</sup>). Furthermore, the cation-exchange-  
335 capacity (CEC) of the sediments buffered some processes in pore water chemistry  
336 by net adsorption of cations at D<sub>1</sub> and net desorption at D<sub>11</sub>.

337 The processes described above occurred in all three sediments, **although**  
338 **oxidation was higher in Mud<sub>soft</sub> than in Mud<sub>sand</sub> and Clay, probably because higher**  
339 **evaporation rates in Mud<sub>soft</sub> enhanced oxidation and affected other reactants related**  
340 **to oxidation.**

341

### 342 3.3.2 Phase 2: Initial stage of plant growth (t = 22–64 days)

343 While the pore water compositions did not show clear differences between unplanted  
344 and planted conditions **during the initial stage of plant growth**, the inverse modeling  
345 provided clear evidence for differences at D<sub>1</sub>. However, chemical differences

346 between unplanted and planted conditions for Mud<sub>sand</sub> might simply be attributed to  
347 concentration/dilution due to H<sub>2</sub>O loss/gain (-996 to 380 mmol l<sup>-1</sup> day<sup>-1</sup>).

348 Overall, more pyrite was oxidized in the planted conditions, though the rates are  
349 much lower than in the first phase (0–64.3 μmol l<sup>-1</sup> day<sup>-1</sup>). This observation provides  
350 evidence that plants may enhance pyrite oxidation by radial oxygen loss (i.e. root  
351 aeration). Ferric oxide production on pyrite surfaces probably impeded further  
352 oxidation of pyrite, which is a common phenomenon in carbonate-buffered conditions  
353 (Nicholson et al., 1990). Indeed, the total pyrite that had oxidized after 64 days (6.3  
354 mmol for Mud<sub>soft</sub>, 2.5 mmol for Mud<sub>sand</sub> and 6.2 mmol for Clay, calculated from the  
355 rates presented in Table 3) corresponds to a small fraction of total pyrite present (50  
356 mmol).

357 Saturation with gypsum led to precipitation of SO<sub>4</sub> and Ca at D<sub>1</sub>. Table 3 shows  
358 that with the exception of Mud<sub>sand</sub>, mole transfers were lower for planted conditions;  
359 the probable reason is that citric acid production by root tips retarded gypsum  
360 precipitation (Prisciandaro et al., 2005). This process was not relevant at D<sub>11</sub>, as  
361 here aeration (and subsequent sulfate production) by plant roots was minor (in the  
362 case of Clay) or absent (in the case of Mud<sub>soft</sub> and Mud<sub>sand</sub>).

363 The thin moss layer that started to develop after several weeks in the unplanted  
364 condition on top of the Mud<sub>soft</sub> sediment slowed down the aeration rate to 2.62 μmol  
365 l<sup>-1</sup> day<sup>-1</sup> and might be the reason for the moderate increase in P, which probably  
366 resulted from Fe(OH)<sub>3</sub> dissolution (0.95 μmol l<sup>-1</sup> day<sup>-1</sup>) (Figure 1g, Table 3).

367

368 3.3.3 Phase 3: Root influence (t = 64–176 days)

369 Phase 3 took place in the autumn, when temperatures were lower and therefore the  
370 soils did not dry out; hence there was a net gain in H<sub>2</sub>O. The gain was less in planted  
371 conditions, due to uptake of water by roots.

372 The fully grown plants continued to influence pore water chemistry at D<sub>1</sub>, but in the  
373 unplanted conditions the chemical changes were minor (Table 3). Radial oxygen loss  
374 continued the oxidation processes described in the previous sections. It should be  
375 noted that *P. australis* is known to have higher radial oxygen loss than other wetland  
376 species (Brix et al., 1996; Dickopp et al., 2011; Smith and Luna, 2013), so the  
377 aeration effect found in this study cannot be assumed to hold for other species.

378 In contrast to the previous phase, in phase 3 the influence of roots was clearly  
379 visible at D<sub>11</sub> for all three sediments. All planted sediments showed increased  
380 aeration and subsequent oxidation of pyrite due to radial oxygen loss, with a notable  
381 difference between Mud<sub>soft</sub> (lower) and Mud<sub>sand</sub> (higher). This is somewhat surprising,  
382 as the belowground biomass was significantly higher in Mud<sub>soft</sub> (section 3.4). It  
383 indicates that increasing the average grain size by adding sand enhanced aeration,  
384 even when root biomass production was low.

385

### 386 *3.4 Plant response*

387 Above- and belowground biomass were significantly higher in Mud<sub>soft</sub> and Clay than  
388 in Mud<sub>sand</sub> (Figure 3;  $p < 0.02$ ). The difference between the two Mud sediments  
389 cannot be explained by nutrient concentrations in pore water or light conditions in the  
390 greenhouse, as these were the same for the two sediments. As biomass production  
391 in Mud<sub>sand</sub> was not limited by chemical or biological properties relative to Mud<sub>soft</sub>, it  
392 seems likely that the reason for the lower biomass production in Mud<sub>sand</sub> is a  
393 difference in physical properties. Voorhees et al. (1975) and Bengough and Mullins



394 (1990) showed that so-called mechanical impedance (i.e. the resistance to  
395 penetration by the root tip) was higher in loamy sand than in clay, which was  
396 attributed to the higher bulk density of the loamy sand. Therefore, increasing the bulk  
397 density of Mud<sub>soft</sub> by mixing with sand increased the mechanical impedance and this  
398 might explain the lower biomass production we observed in Mud<sub>sand</sub>.

399 *P. australis* invested more in its root system than in its shoots and leaves for all  
400 sediments (Figure 3;  $p < 0.01$ ). More investment in roots implies a limitation of N, P,  
401 and/or S (Ericsson, 1995; Shipley and Meziane, 2002). Figures 1a–i and 2d–f show  
402 that the N and P concentrations were indeed low in the planted conditions but that  
403 SO<sub>4</sub> was high, which rules out S limitation. During the experiment, we had observed  
404 reduced plant growth and shriveling and yellowing of foliage 2 months after  
405 transplantation, which might have been caused by nutrient limitation.

406 Figure 4 shows the N, P, and K contents as well as the N:P ratio for the roots of *P.*  
407 *australis* at the beginning and end of the experiment for the three sediment types.  
408 The N, P, and K contents in the roots increased in time, while the N:P ratio clearly  
409 decreased. The reduction in N:P ratio from 11 to 2–3 suggests N was the limiting  
410 nutrient as an N:P ratio of  $< 14$  in plant tissue is indicative of N limitation  
411 (Koerselman and Meuleman, 1996). However, root N and P concentrations of *P.*  
412 *australis* should typically range between 0.64–1.04% for N and 0.06–0.13% for P  
413 (Wang et al., 2015). Figure 4 shows that the root N and P concentrations were above  
414 these values, and that P was particularly high: by a factor of 5 to 10 (N: 1.14–1.63%  
415 and P: 0.52–0.62%). Hence the concentrations of these nutrients in the roots do not  
416 indicate that nutrient limitation is a likely cause of the reduced plant growth and  
417 shriveling and yellowing of foliage.

418 We hypothesize that co-precipitation of P with Fe on roots enhanced the  
419 concentrations of P in the plant roots (Snowden and Wheeler, 1995; Jørgenson et  
420 al., 2012). Snowden and Wheeler (1995) showed that this so-called iron plaque  
421 formation enhances uptake of Fe and P. This may cause iron toxicity and is probably  
422 responsible for the elevated P concentrations in tissue, and for the stunted growth  
423 and leaf decay we observed in the experiment. Note that the plant roots of *P.*  
424 *australis* initiate this process by oxidizing their environment and thereby enabling  
425 ferrous iron to oxidize into P-bearing ferric iron, which precipitates on roots.

426 The Fe concentration in the leaves and in the roots supports the “Fe-P co-  
427 precipitation hypothesis”: we measured an approximately 20-fold increase by  
428 comparison with the initial concentration in the seedlings (Figure 5). Furthermore,  
429 ferric oxide, a product of pyrite oxidation, precipitates on root surfaces (Jørgenson et  
430 al., 2012), and hence pyrite oxidation in sediments is directly linked to iron toxicity in  
431 plants.

432 Further evidence to support our hypothesis is provided by the results of the  
433 sequential phosphorus extraction conducted on the sediments: it revealed that the  
434 dominant P pool in the sediments is the Fe-P fraction (Table 2). P co-precipitates  
435 with Fe on roots if it is bound to ferric oxides.

436

### 437 *3.5. Implications for eco-engineering*

438 Our results strongly point in the direction of iron toxicity as a major bottleneck  
439 prohibiting healthy development of *P. australis*. Since the candidate material for the  
440 construction of the Markermeer wetland has high contents of Fe and Fe-P, we  
441 recommend using Fe-tolerant plant species as test species in the new wetland,  
442 rather than species optimized for growing in N-limited conditions.

443 Concomitantly with iron toxicity, a high Fe-P content in soil will trigger P  
444 mobilization if that soil is rewetted after having dried out and contains high amounts  
445 of SO<sub>4</sub> (Smolders and Roelofs, 1993; Lucassen et al., 2005). In some cases, this can  
446 result in elevated levels of sulfide, thereby promoting S toxicity in plants (Lamers et  
447 al., 1998; Van der Welle et al., 2007).

448 Figure 6 summarizes the important feedbacks and processes we expect play an  
449 important role in the clay-rich sediments. Following the feedback loops between  
450 plant and soil, we see a negative feedback loop that arises because plant roots  
451 induce aeration, which promotes iron toxicity that decreases plant growth and results  
452 in plant death. Also, we see a positive feedback loop, as iron toxicity induces  
453 reduction processes as a result of root death, which leads to P mobilization and  
454 hence enhances plant growth and regeneration. Negative feedback loops diminish or  
455 buffer changes, whereas a positive feedback loop amplifies changes. So, a negative  
456 feedback loop normally stabilizes the system, in our case via the toxic effect of iron  
457 oxides on plants, but plant growth may increase due to the positive feedback loop via  
458 P mobilization. The relative strengths of these two feedback loops and the sensitivity  
459 of species to Fe toxicity determine the ultimate effect on vegetation development in  
460 wetlands built from these sediments.

461 As drying–rewetting cycles are likely to occur in these future wetlands and since  
462 the Fe-P concentrations in the **situated sediment** are high, these feedbacks might be  
463 an important factor influencing soil formation and ecosystem development. We  
464 therefore recommend studying the ultimate effects of the use of this material on  
465 ecosystem development by testing with various plant species and drying–rewetting  
466 cycles.

467 Not all environmental factors that potentially interfere with the processes and  
468 feedbacks described in this study could be taken into account with this experimental  
469 design (e.g. wave action, wind). Therefore, we recommend to carry out experiments  
470 on the wetlands themselves once the crest has stabilized sufficiently.

471

472

#### 473 **4. Conclusions**

474 The results of this study show that plants expedite biogeochemical processes by  
475 oxidizing and modifying their environment, which in turn affects the growth conditions  
476 of the plants. In the mud deposits from Markermeer, the key processes influencing  
477 pore water chemistry are pyrite oxidation and associated calcite dissolution. The  
478 former is especially likely to be important as it is linked to iron toxicity and P  
479 mobilization and thus has the potential to initiate two feedback mechanisms between  
480 plant and soil. We found strong indications for a negative feedback loop, where  
481 plant-induced iron toxicity is hampering plant growth, and a positive feedback loop,  
482 where iron toxicity promotes P mobilization, **enhancing** plant growth. The strength of  
483 these feedbacks and the balance between them will play an important role in  
484 regulating eco-engineering conditions for plants.

485 We found conclusive evidence that the low N:P ratio found in plant tissue was not  
486 caused by N limitation, as the ratio suggests, but probably results from enhanced P  
487 uptake as a result of co-precipitation with Fe on roots.

488 The magnitudes of the feedback mechanisms **are** expected to differ between the  
489 **sediments** used. The soft clay-rich layer has less Fe-P than the underlying clay layer  
490 and therefore P mobilization is expected to be less in mud. However, when the mud  
491 is mixed with sand, the enhanced aeration due to the change in grain-size

492 composition results in higher oxidation rates, increasing the impact of the positive  
493 feedback mechanisms involving P mobilization and iron toxicity.

494 To study the effects of iron toxicity and P mobilization in greater detail, we  
495 recommend further testing with different plant species and drying–rewetting cycles.  
496 This is important because we expect these mechanisms to influence soil formation  
497 and ecosystem development in the created wetlands.

498

#### 499 **Acknowledgements**

500 This study was supported with funding from Netherlands Organization for Scientific  
501 Research (NWO), project no. 850.13.032 and the companies Boskalis and Van  
502 Oord. We would also like to thank Botanical Garden Utrecht for their help, support  
503 and advice during the greenhouse experiment. Joy Burrough advised on the English.  
504 Last, we would like to thank Ingrid Bauer and an anonymous referee for helpful  
505 comments on the manuscript.

506 **References**

- 507 Bauer, A., Velde, B.D.: Soils: Retention and Movement of Elements at the Interface,  
508 in: Geochemistry at the Earth's Surface: Movement of Chemical Elements, Springer-  
509 Verlag Berlin Heidelberg, New York, 2014.
- 510
- 511 Belkhir, L., Boudoukha, A., Mouni, L., Baouz, T.: Application of multivariate statistical  
512 methods and inverse geochemical modeling for characterization of groundwater — A  
513 case study: Ain Azel plain (Algeria), *Geoderma*, 159, 390-398, 2010.
- 514
- 515 Bengough, A.G., Mullins, C.E.: Mechanical impedance to root growth: a review of  
516 experimental techniques and root growth responses, *Journal of Soils Science*, 41,  
517 341-358, 1990.
- 518
- 519 Borsje, B.W., Van Wesenbeeck, B.K., Dekker, F., Paalvast, P., Bouma, T.J., Van  
520 Katwijk, M., De Vries, M.B.: How ecological engineering can serve in coastal  
521 protection, *Ecological Engineering*, 37, 113-122, 2011.
- 522
- 523 Bradford, M.A., Keiser, A.D., Davies, C.A., Mersmann, C.A., Strickland, M.S.:  
524 Empirical evidence that soil carbon formation from plant inputs is positively related to  
525 microbial growth, *Biogeochemistry*, 113, 271-281, 2013.
- 526
- 527 Brix, H., Borrell, B.K., Schierup, H.H.: Gas fluxes achieved by in situ convective flow  
528 in *Phragmites australis*, *Aquatic Botany*, 54, 151-163, 1996.
- 529
- 530 Canavan, R.W., Van Cappellen, P., Zwolsman J.J.G., Van den Berg, G.A., Slomp,  
531 C.A.: Geochemistry of trace metals in a fresh water sediment: Field results and  
532 diagenetic modeling, *Science of the Total Environment*, 381, 263–279, 2007.
- 533
- 534 Carucci, V., Petitta, M., Aravena, R.: Interaction between shallow and deep aquifers  
535 in the Tivoli Plain (Central Italy) enhanced by groundwater extraction: A multi-isotope  
536 approach and geochemical modeling, *Applied Geochemistry*, 27, 266-280, 2012.
- 537
- 538 De Lucas Pardo, M.A., Bakker, M., Van Kessel, T., Cozzoli, F., Winterwerp, J.C.:  
539 Erodibility of soft freshwater sediments in Markermeer: the role of bioturbation by  
540 meiobenthic fauna, *Ocean Dynamics*, 63, 1137-1150, 2013.
- 541
- 542 De Lucas Pardo, M.A.: Effect of biota on fine sediment transport processes. A study  
543 of lake Markermeer, Ph.D thesis, Delft University, the Netherlands, 211 pp., 2014.
- 544
- 545 Dickopp, J., Kazda, M., Cízková, H.: Differences in rhizome aeration of *Phragmites*  
546 *australis* in a constructed wetland, *Ecological Engineering*, 37, 1647-1653, 2011.
- 547

548 Ehrenfeld, J.G., Ravit, B., Elgersma, K.: Feedback in the plant-soil system, Annual  
549 Review of Environment and Resources, 30, 75-115, 2005.  
550  
551 Ericsson, T.: Growth and shoot:root ratio of seedlings in relation to nutrient  
552 availability, Plant and Soil, 168, 205-214, 1995.  
553  
554 Gerke, J., Beissner, L., Römer W.: The quantitative effect of chemical phosphate  
555 mobilization by carboxylate anions on P uptake by a single root. I. The basic concept  
556 and determination of soil parameters, Journal of Plant Nutrition and Soil Science,  
557 163, 207-212, 2000.  
558  
559 Holtkamp, R., Van der Wal, A., Kardol, P., Van Putten, W.H., De Ruiter, P.C.,  
560 Dekker, S.C.: Modelling C and N mineralisation in soil food webs during secondary  
561 succession on ex-arable land, Soil Biology and Biochemistry, 43, 251-260, 2011.  
562  
563 Howard, P.J.A.: The Carbon-Organic Matter Factor in Various Soil Types, Oikos, 15,  
564 229-236, 1965.  
565  
566 Jilbert, T., Slomp C.P.: Iron and manganese shuttles control the formation of  
567 authigenic phosphorus minerals in the euxinic basins of the Baltic Sea, Geochimica  
568 et Cosmochimica Acta, 107, 155–169, 2013.  
569  
570 Jones, C.G., Lawton, J.H., Shachak, M.: Organisms as Ecosystem Engineers, Oikos,  
571 69, 373-386, 1994.  
572  
573 Jørgenson, K.D., Lee, P.F., Kanavillil, N.: Ecological relationships of wild rice,  
574 *Zizania* spp. 11. Electron microscopy study of iron plaques on the roots of northern  
575 wild rice (*Zizania palustris*), Botany, 91, 189–201, 2012.  
576  
577 Koerselman, W., Meuleman, A.F.M.: The vegetation N:P ratio: a new tool to detect  
578 the nature of nutrient limitation, Journal of Applied Ecology, 33, 1441-1450, 1996.  
579  
580 Lambers, H., Mougél, C., Jaillard, B., Hinsinger P.: Plant-microbe-soil interactions in  
581 the rhizosphere: an evolutionary perspective, Plant and Soil, 321, 83-115, 2009.  
582  
583 Lamers, L.P.M., Tomassen, H.B.M., Roelofs J.G.M.: Sulfate-Induced Eutrophication  
584 and Phytotoxicity in Freshwater Wetlands, Environmental Science and Technology,  
585 32, 199-205, 1998.  
586  
587 Lecomte, K.L., Pasquini, A.I., Depetris, P.J.: Mineral weathering in a Semiarid  
588 Mountain River: Its assessment through PHREEQC inverse modeling, Aquatic  
589 Geochemistry, 11, 173-194, 2005.  
590

591 LMRe (Landelijk Meetnet Regenwater): <http://www.lml.rivm.nl/gevalideerd/>, last  
592 access: 17 November 2014, 2014.  
593

594 Lucassen, E.C.H.E.T., Smolders, A.J.P., Lamers, L.P.M., Roelofs, J.G.M.: Water  
595 table fluctuations and groundwater supply are important in preventing phosphate-  
596 eutrophication in sulphate-rich fens: Consequences for wetland restoration, *Plant  
597 and Soil*, 269, 109-115, 2005.  
598

599 Nicholson, R.V., Gillham, R.W., Reardon E.J.: Pyrite oxidation in carbonate-buffered  
600 solution: 2. Rate control by oxide coatings, *Geochimica et Cosmochimica Acta*, 54,  
601 395-402, 1990.  
602

603 Noordhuis, R., Groot, S., Dionisio Pires, M., Maarse M.: Wetenschappelijk  
604 eindadvies ANT-IJsselmeergebied. Vijf jaar studie naar kansen voor het ecosysteem  
605 van het IJsselmeer, Markermeer en IJmeer met het oog op de Natura-2000 doelen,  
606 Open File Rep. 1207767-000, 98 pp., 2014.  
607

608 Olde Venterink, H.: Does phosphorus limitation promote species-rich plant  
609 communities?, *Plant and Soil*, 345, 1-9, 2011.  
610

611 O'Kelly, B.C.: Compression and consolidation anisotropy of some soft soils,  
612 *Geotechnical and Geological Engineering*, 24, 1715-1728, 2006.  
613

614 Onipchenko, V.G., Makarov, M.I., Van der Maarel, E.: Influence of alpine plants on  
615 soil nutrient concentrations in a monoculture experiment, *Folia Geobotanica*, 36,  
616 225-241, 2001.  
617

618 Parkhurst, D.L., Appelo, C.A.J.: Description of input and examples for PHREEQC  
619 version 3-A computer program for speciation, batch-reaction, one-dimensional  
620 transport, and inverse geochemical calculations, U.S. Geological Survey, Denver,  
621 497 pp., 2013.  
622

623 Prisciandaro, M., Santucci, A., Lancia, A., Musmarra, D.: Role of citric acid in  
624 delaying gypsum precipitation, *The Canadian journal of Chemical Engineering*, 83,  
625 586-592, 2005.  
626

627 Ruttenberg, K.C.: Development of a sequential extraction method for different forms  
628 of phosphorus in marine sediments, *Limnology Oceanography*, 37, 1460-1482, 1992.  
629

630 Shipley, B., Meziane D.: The balanced-growth hypothesis and the allometry of leaf  
631 and root biomass allocation, *Functional Ecology*, 16, 326-331, 2002.  
632



633 Smith, K.E., Luna, T.O.: Radial Oxygen Loss in Wetland Plants: Potential Impacts on  
634 Remediation of Contaminated Sediments, *Journal of Environmental Engineering*,  
635 139, 496-501, 2013.

636

637 Smolders, A., Roelofs J.G.M.: Sulphate-mediated iron limitation and eutrophication in  
638 aquatic ecosystems, *Aquatic Botany*, 46, 247-253, 1993.

639

640 Snowden, R.E.D., Wheeler, B.D.: Chemical changes in selected wetland plant  
641 species with increasing Fe supply, with specific reference to root precipitates and Fe  
642 tolerance, *New Phytologist*, 131, 503-520, 1995.

643

644 Taylor, L.L., Leake, J.R., Quirk, J., Hardy, K., Banwart, S.A., Beerling, D.J.:  
645 Biological weathering and the long-term carbon cycle: integrating mycorrhizal  
646 evolution and function into the current paradigm, *Geobiology*, 7, 171-191, 2009.

647

648 Temmerman, S., Meire, P., Bouma, T.J., Herman, P.M.J., Ysebaert, T., De Vriend,  
649 H.K.: Ecosystem-based coastal defence in the face of global change, *Nature*, 504,  
650 79-83, 2013.

651

652 Van der Welle, M.E.W., Smolders, A.J.P., Op den Camp, H.J.P., Roelofs, J.G.M.,  
653 Lamers, L.P.M.: Biogeochemical interactions between iron and sulphate in  
654 freshwater wetlands and their implications for interspecific competition between  
655 aquatic macrophytes, *Freshwater Biology*, 52, 434-447, 2007.

656

657 Van Hees, P.A.W., Jones, D.L., Finlay, R., Godbold, D.L., Lundström U.S.: The  
658 carbon we do not see—the impact of low molecular weight compounds on carbon  
659 dynamics and respiration in forest soils: a review, *Soil Biology and Biochemistry*, 37,  
660 1-13, 2005.

661

662 Van Kessel, T., De Boer, G., Boderie P.: Calibration suspended sediment model  
663 Markermeer, Open File Rep. 4612, 107 pp., 2008.

664

665 Vijverberg, T., Winterwerp, J.C., Aarninkhof, S.G.J., Drost, H.: Fine sediment  
666 dynamics in a shallow lake and implication for design of hydraulic works, *Ocean  
667 Dynamics*, 61, 187-202, 2011.

668

669 Voorhees, W.B., Farrel, D.A., Larson, W.E.: Soil strength and aeration effects on root  
670 elongation, *Soil Science Society of America Journal*, 39, 948-953, 1975.

671

672 Wang, W.Q., Sardans, J., Wang, C., Zeng, C.S., Tong, C., Asensio, D., Penuelas, J.:  
673 Ecological stoichiometry of C, N, and P of invasive *Phragmites australis* and native  
674 *Cyperus malaccensis* species in the Minjiang River tidal estuarine wetlands of China,  
675 *Plant Ecology*, 216, 809-822, 2015.

676 **Table 1.** List of steps used in the extraction procedure of phosphorus (based on  
 677 Ruttenberg, 1992).

<b>Step</b>	<b>Extractant</b>	<b>Separated P fraction</b>
I	1M MgCl <sub>2</sub> , 30 min	Exchangeable or loosely sorbed P
II	A Citrate-dithionite-bicarbonate (CDB), 8 h	Easily reducible or reactive ferric Fe- P
	B 1M MgCl <sub>2</sub> , 30 min	
III	A Na acetate buffer (pH 4), 6 h	Amorphous apatite and carbonate P
	B 1M MgCl <sub>2</sub> , 30 min	
IV	1M HCl, 24 h	Crystalline apatite and other inorganic P
V	Ash at 550 °C, 2h; 1M HCl, 24 h	Organic P

678 **Table 2.** Geochemical and mineralogical composition of the sediment types used in  
 679 this study. Significant differences between Mud<sub>soft</sub> and Clay are indicated by \* (p <  
 680 0.05).

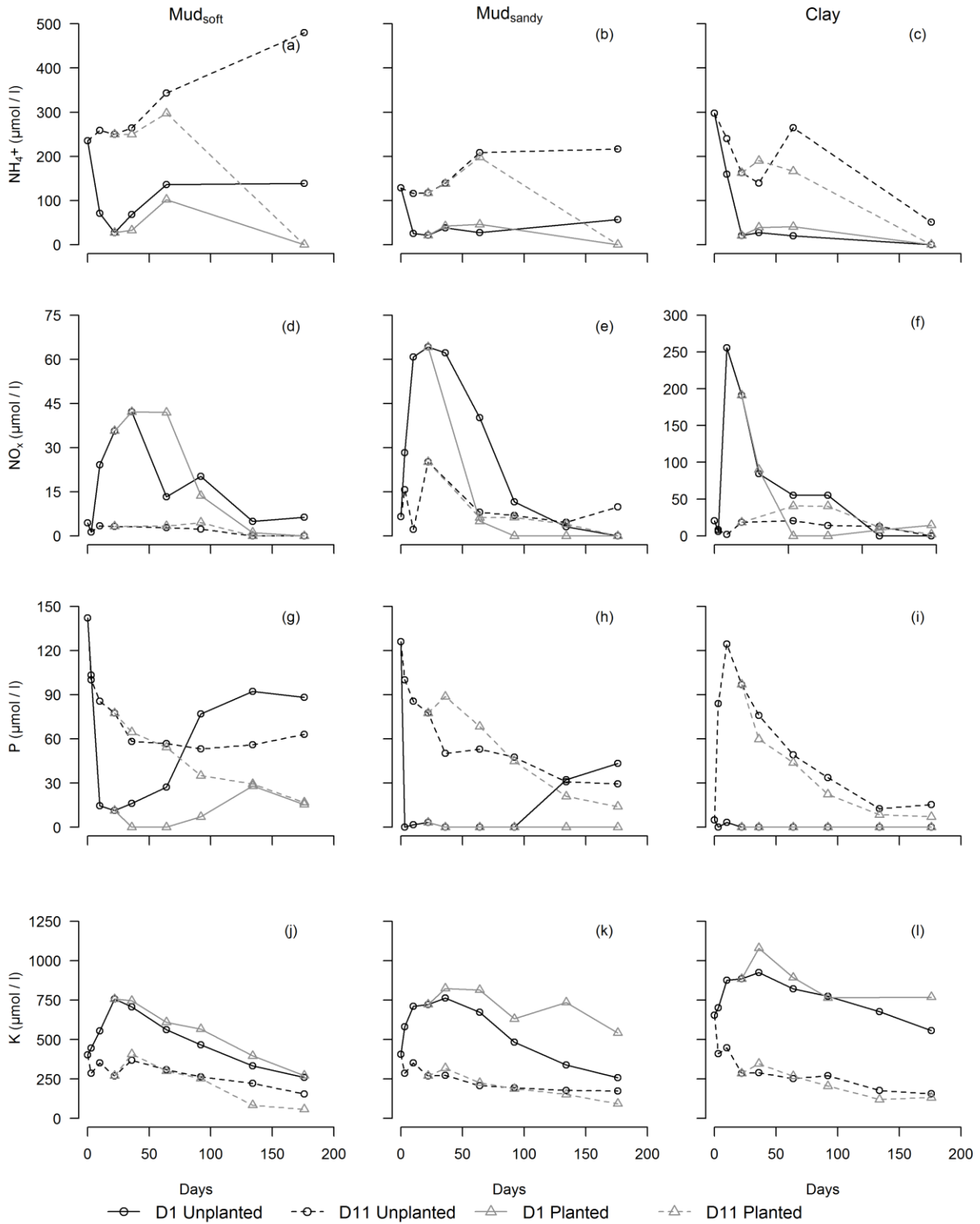
	Unit	n per type	Clay Mean	SD	Mud <sub>soft</sub> Mean	SD	Mud <sub>sand</sub> Mean	SD
<i>Aqua regia / CS</i>								
<b>Al*</b>	mg/kg	15	21989	4512	16593	3130	6394	2439
<b>Ca</b>	mg/kg	15	48031	3032	45635	6020	18877	3572
<b>Fe*</b>	mg/kg	15	27766	3764	20745	2987	7804	2281
<b>K</b>	mg/kg	15	5371	1262	4102	641	1723	742
<b>Mg*</b>	mg/kg	15	8041	1017	6636	906	2531	558
<b>Mn*</b>	mg/kg	15	710	166	577	160	238	62
<b>Na*</b>	mg/kg	15	992	379	526	158	219	64
<b>P*</b>	mg/kg	15	1186	217	649	169	259	56
<b>S</b>	mg/kg	15	5727	710	5586	698	3001	846
<b>Sr</b>	mg/kg	15	148	21	135	26	62	14
<b>Ti</b>	mg/kg	15	312	74	312	77	125	44
<b>Zn*</b>	mg/kg	15	159	58	110	29	43	18
<i>Seq. P extraction</i>								
<b>Exchangeable P</b>	mg/kg	15	14.3	6.81	11.9	3.50	5.9	1.79
<b>Fe- bound P*</b>	mg/kg	15	772	263	279	61.7	94.5	29.0
<b>Ca-bound P</b>	mg/kg	15	146	43.3	121	30.9	36.8	13.1
<b>Detrital P</b>	mg/kg	15	147	16.5	169	14.1	51.5	10.9
<b>Organic P</b>	mg/kg	15	99.6	20.0	117	25.1	47.7	8.38
<i>XRD</i>								
<b>Quartz</b>	%	1	48		37		n.a.	
<b>Calcite</b>	%	1	9		9		n.a.	
<b>Pyrite</b>	%	1	0.6		0.6		n.a.	
<b>Illite</b>	%	1	15		21		n.a.	
<b>Smectite</b>	%	1	11		14		n.a.	
<b>Kaolinite</b>	%	1	3		5		n.a.	
<b>Chlorite</b>	%	1	2		3		n.a.	
<i>Other</i>								
<b>Organic matter</b>	%	5	6.7	0.6	7.2	0.6	2.8	0.4
<b>CEC (calculated)</b>	meq/100g		30.0		37.2		12.4	

681

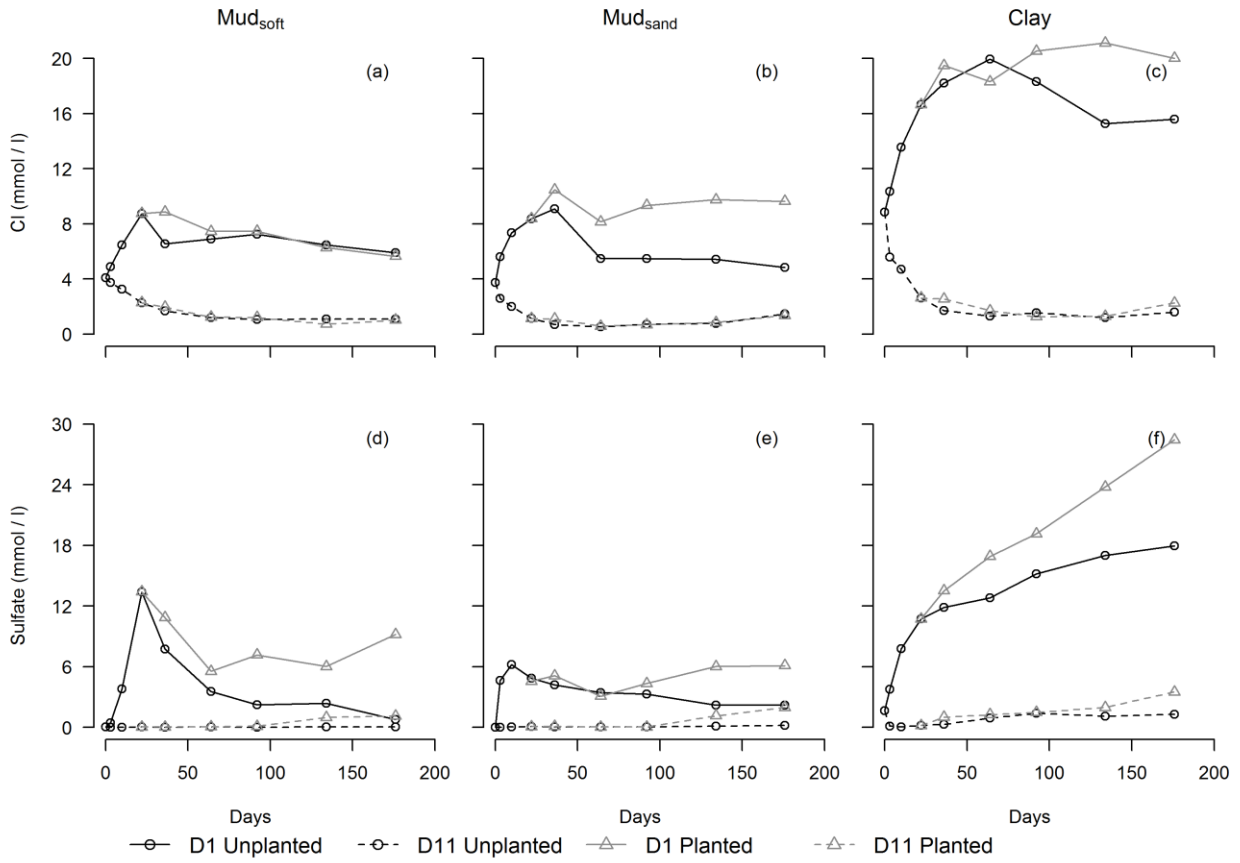
682 **Table 3.** Main pore water processes expressed in mole transfers ( $\mu\text{mol l}^{-1} \text{ day}^{-1}$ ) as modeled by PHREEQC with pore water data  
683 retrieved at 1 cm and 11 cm below sediment surface ( $D_1$  and  $D_{11}$  respectively). Positive values indicate dissolution, negative values  
684 indicate precipitation. Cation exchange capacity (CEC) is the sum of Ca, Fe, K, Mg, Na, and  $\text{NH}_4$ .

Phase	Condition	Calcite		Gypsum		$\text{Fe}(\text{OH})_3$		Pyrite		$\Sigma\text{CEC}$		$\text{H}_2\text{O} (\times 10^3)$		$\text{O}_2$	
		$D_1$	$D_{11}$	$D_1$	$D_{11}$	$D_1$	$D_{11}$	$D_1$	$D_{11}$	$D_1$	$D_{11}$	$D_1$	$D_{11}$	$D_1$	$D_{11}$
<b>1. Oxidation</b> <b>t=0-22 days</b>	<b>Mud<sub>soft</sub></b> <b>No plant</b>	267	111	0.00	-72.5	-277	0.00	270	36.2	-31.3	20.2	-3364	0.00	1009	119
	<b>Mud<sub>sand</sub></b> <b>No plant</b>	0.00	59.6	0.00	-40.7	-116	0.00	109	21.7	-4.99	7.92	-2591	0.00	432	69.5
	<b>Clay</b> <b>No plant</b>	120	55.2	0.00	-53.4	-160	0.00	159	20.1	-91.4	14.0	-2364	0.00	659	61.9
<b>2. Initial root development</b> <b>t=22-64 days</b>	<b>Mud<sub>soft</sub></b> <b>No plant</b>	27.1	0.00	-236	0.00	0.95	-0.24	0.00	0.00	-23.1	1.43	0.00	0.00	2.62	0.00
	<b>Mud<sub>soft</sub></b> <b>Plant</b>	48.8	19.8	-208	-3.81	-10.0	-6.19	9.76	0.00	-7.63	1.43	0.00	0.00	45.5	0.00
	<b>Mud<sub>sand</sub></b> <b>No plant</b>	39.3	71.7	0.00	0.00	0.00	-41.2	0.21	0.00	1.90	1.46	380	0.00	0.00	0.00
	<b>Mud<sub>sand</sub></b> <b>Plant</b>	7.10	83.8	-83.4	0.00	0.00	-51.2	3.58	0.00	5.40	3.40	-996	0.00	0.00	0.00
	<b>Clay</b> <b>No plant</b>	0.00	27.1	-32.1	0.00	-21.4	-25.0	21.2	0.00	0.01	-0.23	-286	0.00	41.9	0.00
<b>Clay</b> <b>Plant</b>	36.9	16.2	0.00	0.00	-14.3	0.00	64.3	11.9	28.4	4.53	-6.67	0.00	186	40.5	
<b>3. Root influence</b> <b>t=64-176 days</b>	<b>Mud<sub>soft</sub></b> <b>No plant</b>	0.00	-3.21	-19.2	0.00	-1.34	-0.80	0.00	0.00	-1.07	-1.43	56.3	0.00	0.00	0.00
	<b>Mud<sub>soft</sub></b> <b>Plant</b>	25.8	0.00	0.00	0.00	-4.20	0.00	23.8	4.11	7.88	-4.65	49.1	0.00	83.6	13.6
	<b>Mud<sub>sand</sub></b> <b>No plant</b>	8.13	0.00	-7.59	0.00	-10.6	-1.34	0.00	0.00	-1.78	1.42	74.1	0.00	0.00	0.00
	<b>Mud<sub>sand</sub></b> <b>Plant</b>	0.00	0.00	-14.8	0.00	-13.3	-23.2	13.8	7.95	0.12	-10.6	-357	-652	44.7	32.6
	<b>Clay</b> <b>No plant</b>	0.00	11.5	0.00	0.00	0.00	-13.8	33.3	0.00	23.9	0.36	134	0.00	113	0.00
<b>Clay</b> <b>Plant</b>	115	18.7	0.00	0.00	-58.5	-8.48	58.3	8.57	45.4	-5.73	0.00	-98.2	215	28.4	

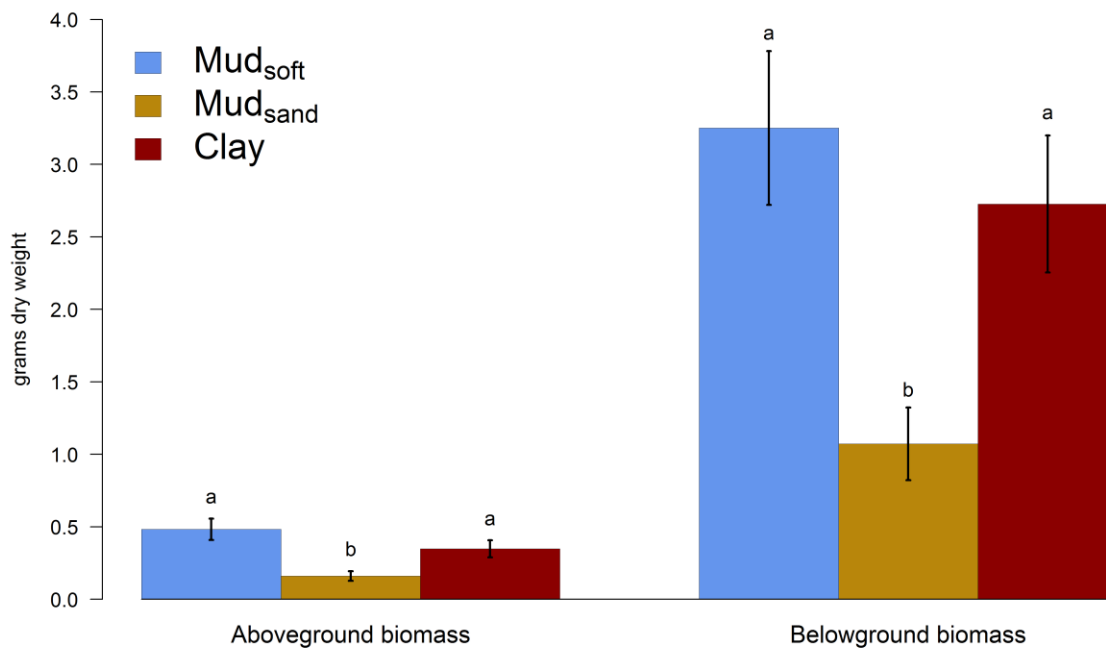
685



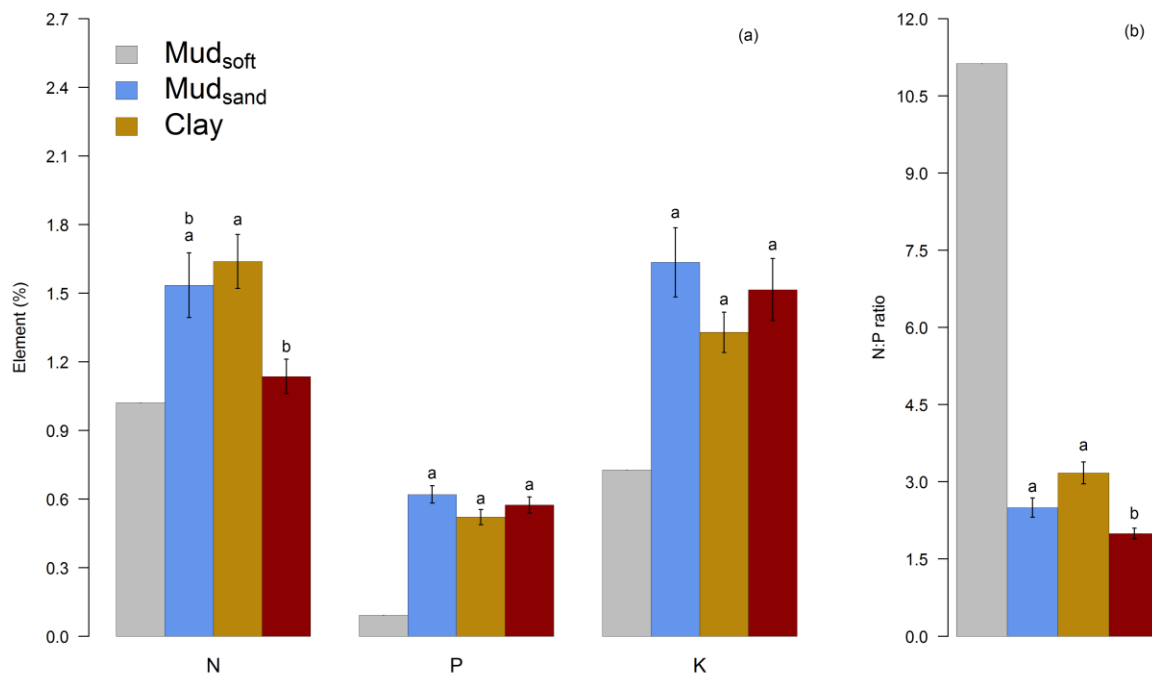
686 **Figure 1.** Time series of NH<sub>4</sub> (a–c), NO<sub>x</sub> (d–f), P (g–i) and K (j–l) concentrations.  
 687 Each column represents one sediment type: Mud<sub>soft</sub> (a, d, g, j), Mud<sub>sandy</sub> (b, e, h, k),  
 688 and Clay (c, f, i, l). The variable and the scale of the x-axis are the same for each  
 689 row, except for the scale in f.



690 **Figure 2.** Time series of Cl (a–c) and sulfate (d–f) concentrations. Each column  
 691 represents one sediment type: Mud<sub>soft</sub> (a, d), Mud<sub>sand</sub> (b, e), and Clay (c, f). The  
 692 variable and the scale of the x-axis are the same for each row.

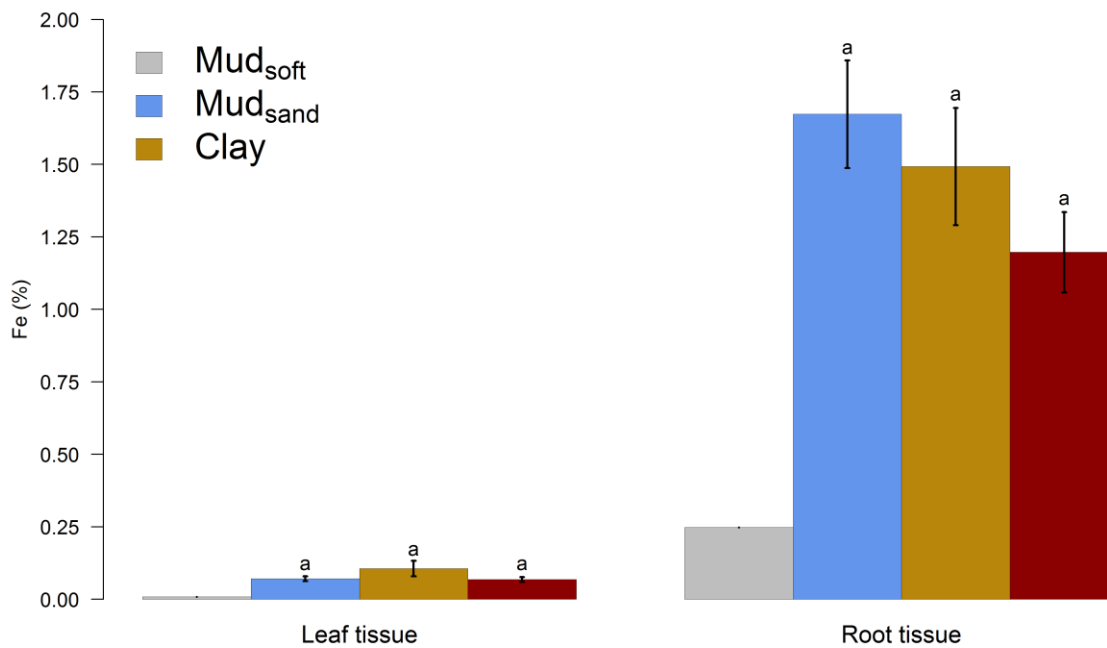


693 **Figure 3.** Above- and belowground biomass in grams dry weight, with error bars (n =  
 694 5). Significant differences between sediment types are indicated by different letters,  
 695 and non-significant differences are indicated by a similar letter.

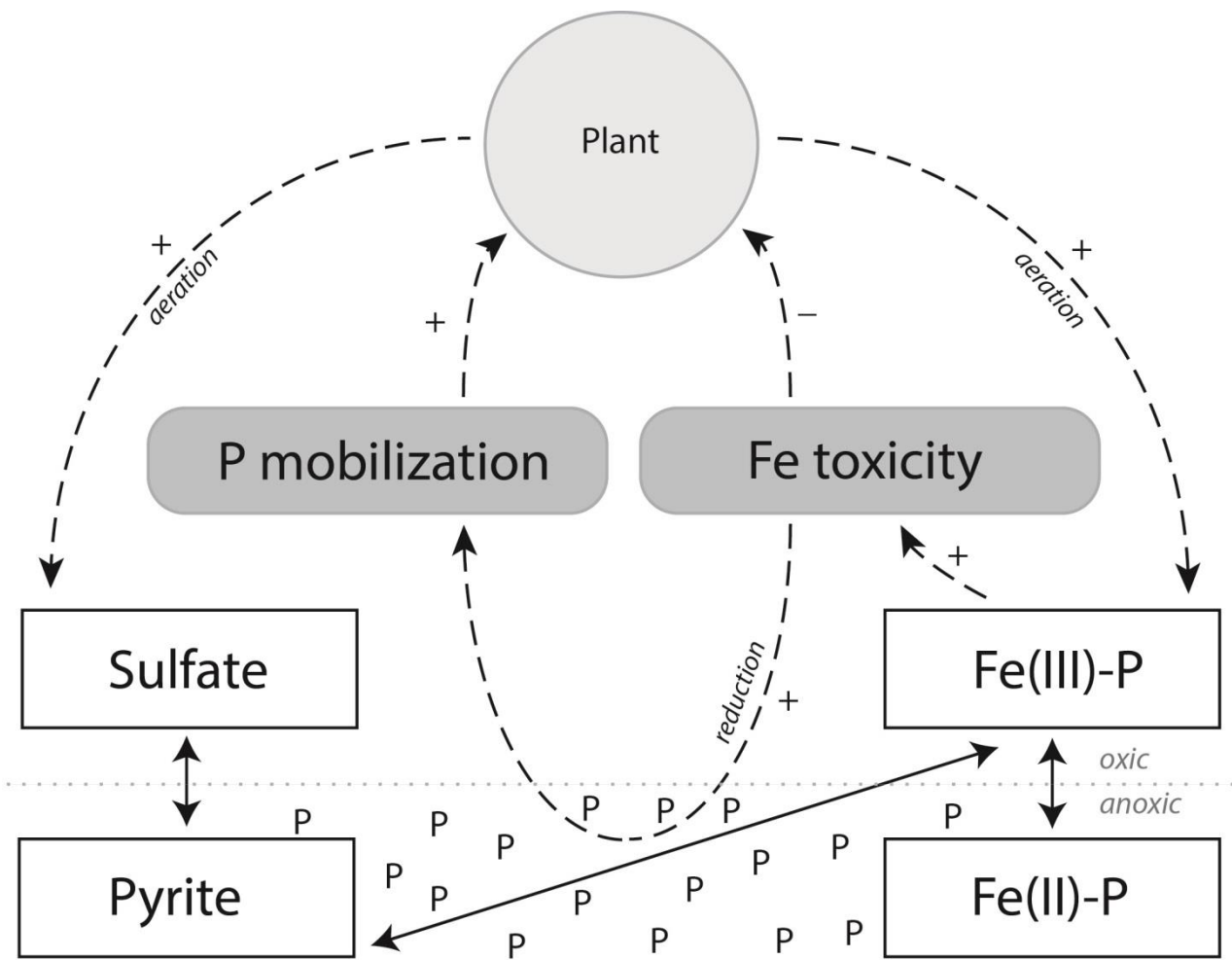


696 **Figure 4.** N, P, and K concentration in root tissue (t = 176) in % of dry weight (a) as  
 697 well as the N:P ratio (b) with error bars when n = 5. Significant differences between  
 698 sediment types are indicated by different letters, and non-significant differences are  
 699 indicated by a similar letter.





700 **Figure 5.** Fe concentration (% of dry weight) in leaf and root tissue with error bars  
 701 when n = 5. Significant differences between sediment types are indicated by different  
 702 letters, and non-significant differences are indicated by a similar letter.



703 **Figure 6.** Most important biogeochemical processes and feedbacks identified in this  
 704 study. + indicates positive feedback, - indicates negative feedback.

705 **Appendix**

706

707 **Table A1.** Pore water processes expressed in mole transfers ( $\mu\text{mol l}^{-1} \text{ day}^{-1}$ ) as modeled by PHREEQC with pore water data  
 708 retrieved at 1 cm below sediment surface. Positive values indicate dissolution, negative values indicate precipitation.

Reactant	Composition	Phase 1. Oxidation (t=0-22)			Phase 2. Initial root development (t=22-64)						Phase 3. Root influence (t=64-176)					
		No plant Mud <sub>soft</sub>	No plant Mud <sub>sand</sub>	No plant Clay	No plant Mud <sub>soft</sub>	Plant	No plant Mud <sub>sand</sub>	Plant	No plant Clay	Plant	No plant Mud <sub>soft</sub>	Plant	No plant Mud <sub>sand</sub>	Plant	No plant Clay	Plant
Calcite	CaCO <sub>3</sub>	267	0.00	120	27.1	48.8	39.3	7.1	0.00	36.9	0.00	25.8	8.13	0.00	0.00	115
Gypsum	CaSO <sub>4</sub> :2H <sub>2</sub> O	0.00	0.00	0.00	-236	-208	0.00	-83.4	-32.1	0.00	-19.2	0.00	-7.59	-14.8	0.00	0.00
Hydroxyapatite	Ca <sub>5</sub> (PO <sub>4</sub> ) <sub>3</sub> (OH)	-5.00	-3.64	0.00	0.24	0.00	-0.02	-0.04	0.00	0.00	0.18	0.00	0.09	0.00	0.00	0.00
Chalcedony	SiO <sub>2</sub>	-19.1	-15.5	-18.2	0.95	0.71	1.91	-3.37	-1.67	-2.14	0.71	0.00	0.54	1.43	0.00	-0.36
Fe(OH) <sub>3</sub> (a)	Fe(OH) <sub>3</sub>	-277	-116	-160	0.95	-10.0	0.00	0.00	-21.4	-14.3	-1.34	-4.20	-10.6	-13.3	0.00	-58.5
Pyrite	FeS <sub>2</sub>	270	109	159	0.00	9.76	0.21	3.58	21.2	64.3	0.00	23.8	0.00	13.8	33.3	58.3
Rhodochrosite	MnCO <sub>3</sub>	-11.8	-11.4	-2.27	2.86	1.19	1.23	0.34	-0.24	-0.24	-0.63	-0.89	0.09	0.18	0.00	0.00
CEC	CaX <sub>2</sub>	0.00	20.9	55.5	63.1	41.9	-9.11	0.00	0.00	0.00	2.50	0.00	-9.73	0.00	-9.64	-85.4
	FeX <sub>2</sub>	0.00	0.00	0.00	0.00	0.00	-0.19	-4.11	0.00	-50.2	1.61	-19.8	11.7	0.00	-33.3	0.00
	KX	-8.64	-5.00	-17.7	-4.76	0.00	3.78	-8.30	-6.19	0.00	-2.14	-2.14	-2.77	-7.68	0.00	0.00
	MgX <sub>2</sub>	31.4	-16.8	36.8	-39.8	-30.5	7.42	-1.35	0.00	21.7	-3.04	12.0	0.00	0.00	19.1	39.8
	NaX	-20.9	0.00	-166	-46.4	-25.7	0.00	25.1	25.2	77.6	0.00	19.7	0.00	12.0	49.4	92.9
	NH <sub>4</sub> X	-33.2	-4.09	0.00	4.76	6.67	0.00	-5.94	-19.0	-20.7	0.00	-1.88	-0.98	-4.20	-1.70	-1.88
H <sub>2</sub> O (g)	H <sub>2</sub> O x 10 <sup>3</sup>	-3364	-2591	-2364	0.00	0.00	380	-996	-286	-6.67	56.3	49.1	74.1	-357	134	0.00
O <sub>2</sub> (g)	O <sub>2</sub>	1009	432	659	2.62	45.5	0.00	0.00	41.9	186	0.00	83.6	0.00	44.7	113	215
CO <sub>2</sub> (g)	CO <sub>2</sub>	-827	-532	-650	35.2	0.00	39.7	0.00	-55.5	-84.8	0.00	-33.1	0.00	44.6	-31.7	-115
No. models found		2	2	2	3	4	2	2	5	2	6	2	1	2	2	1

709

710 **Table A2.** Pore water processes expressed in mole transfers ( $\mu\text{mol l}^{-1} \text{ day}^{-1}$ ) as modeled by PHREEQC with pore water data

711 retrieved at 11 cm below sediment surface. Positive values indicate dissolution, negative values indicate precipitation.

Reactant	Composition	Phase 1. Oxidation (t=0-22)			Phase 2. Initial root development (t=22-64)						Phase 3. Root influence (t=64-176)					
		No plant Mud <sub>soft</sub>	No plant Mud <sub>sand</sub>	No plant Clay	No plant Mud <sub>soft</sub>	Plant	No plant Mud <sub>sand</sub>	Plant	No plant Clay	Plant	No plant Mud <sub>soft</sub>	Plant	No plant Mud <sub>sand</sub>	Plant	No plant Clay	Plant
Calcite	CaCO <sub>3</sub>	111	59.6	55.2	0.00	19.8	71.7	83.8	27.1	16.2	-3.21	0.00	0.00	0.00	11.5	18.7
Gypsum	CaSO <sub>4</sub> :2H <sub>2</sub> O	-72.5	-40.7	-53.4	0.00	-3.81	0.00	0.00	0.00	0.00	0.00	0.00	0.00	0.00	0.00	0.00
Hydroxyapatite	Ca <sub>5</sub> (PO <sub>4</sub> ) <sub>3</sub> (OH)	0.00	0.51	1.45	-0.24	0.00	0.00	0.00	0.00	0.00	0.00	-0.09	0.00	-0.45	0.00	-0.18
Chalcedony	SiO <sub>2</sub>	4.44	5.32	6.74	1.90	3.33	3.10	3.81	1.67	0.95	-0.18	-1.07	-0.27	-3.48	0.00	-1.07
Fe(OH) <sub>3</sub> (a)	Fe(OH) <sub>3</sub>	0.00	0.00	0.00	-0.24	-6.19	-41.2	-51.2	-25.0	0.00	-0.80	0.00	-1.34	-23.2	-13.8	-8.48
Pyrite	FeS <sub>2</sub>	36.2	21.7	20.1	0.00	0.00	0.00	0.00	0.00	11.9	0.00	4.11	0.00	7.95	0.00	8.57
Rhodochrosite	MnCO <sub>3</sub>	0.00	1.18	0.31	0.00	0.48	1.19	0.95	0.00	0.24	0.00	0.00	0.00	-0.71	0.18	0.09
CEC	CaX <sub>2</sub>	0.00	0.00	0.00	-1.43	-5.95	-50.7	-63.3	-7.86	0.00	1.70	8.39	0.00	0.00	-3.75	0.00
	FeX <sub>2</sub>	-35.5	-20.9	-19.0	0.00	0.00	42.4	51.7	0.00	-11.9	1.07	-3.66	-0.54	15.2	4.29	0.00
	KX	7.00	5.87	3.76	0.00	0.00	2.62	2.86	-5.95	1.67	-0.89	-1.79	0.00	-3.84	0.00	-1.70
	MgX <sub>2</sub>	15.4	13.0	4.87	0.00	4.76	7.14	8.57	8.10	7.38	-1.25	0.00	0.00	-4.11	2.59	5.71
	NaX	25.2	9.95	24.4	0.00	0.00	0.00	5.24	0.00	6.43	-4.29	-4.20	1.96	-12.4	0.00	-5.54
	NH <sub>4</sub> X	8.12	0.00	0.00	2.86	2.62	0.00	-1.67	5.48	0.95	2.23	-3.39	0.00	-5.80	-2.77	-4.20
H <sub>2</sub> O (g)	H <sub>2</sub> O x 10 <sup>3</sup>	0.00	0.00	0.00	0.00	0.00	0.00	0.00	0.00	0.00	0.00	0.00	0.00	-652	0.00	-98.2
O <sub>2</sub> (g)	O <sub>2</sub>	119	69.5	61.9	0.00	0.00	0.00	0.00	0.00	40.5	0.00	13.6	0.00	32.6	0.00	28.4
CO <sub>2</sub> (g)	CO <sub>2</sub>	156	0.00	43.0	0.00	0.00	0.00	0.00	0.00	14.5	0.00	0.00	0.00	-67.3	0.00	-13.7
<b>No. models found</b>		2	2	1	4	4	2	2	3	2	1	4	2	4	2	1

712

713